Constraining time-dependent dark energy with the flux power spectrum of the Lyman α forest

G. J. Mathews, J. W. Coughlin, L. A. Phillips, A. P. Snedden and I.-S. Suh

Department of Physics, Center for Astrophysics, University of Notre Dame, Notre Dame, IN 46556, USA
** E-mail: gmathews@nd.edu*
https://physics.nd.edu/people/faculty/grant-j-mathews/

Calculations of the flux power spectrum of the Lyman α forest are performed as a means to quantify the possible effects of time-dependent dark energy. We use a parameterized version of the time-dependent dark energy equation of state consistent with the *Planck* analysis. We have run high-resolution, large-scale cosmological simulation with a modified version of the publicly available SPH code `GADGET-2`. These simulations were used to extract synthetic Lyman α forest spectra. These were then used to simulate the flux power spectrum at various observed quasar redshifts. We conclude that the effect of time-dependent dark energy on the flux power spectrum is of marginal statistical significance compared to the intrinsic cosmic variance.

Keywords: Cosmology: dark energy — cosmology: theory — methods: numerical.

1. Introduction

The origin of the present cosmic acceleration remains a mystery. Within the dark energy paradigm several time-dependent models have been proposed as the physical mechanism for cosmic acceleration.[1]. The simplest model is that of a cosmological constant. Another possibility, however, is a self-coupled, slowly evolving scalar field that manifests as either a cosmic quintessence[2] or k-essence[3]. The empirical difference between the cosmological constant and all other dark energy models is that the energy density of the later can vary in time. Hence, discriminating between various dark energy models can be made by observing how the dark energy changes in time.

Current observational constraints on time-dependent dark energy, however, are quite weak[4]. In the work described here[5] we consider using the Lyman-α forest as a means to constrain the time evolution of dark energy. The motivation for using the Lyman-α forest is that the effects of dark energy, should be most apparent on the morphology of voids in the cosmic web.[6–12] The absorbers responsible for the Lyman-α forest should reside primarily in the clusters and filaments.[13,14] Along the line of sight to distant quasars these absorbers will be separated by the voids. As such, the separation of these absorbers in redshift space should act as a tracer of the evolution of the voids.[15] Hence, the flux power spectrum acts as a proxy for the matter power spectrum and should contain complementary information about how each dark energy model affects the expansion of the universe. Thus, studying the Lyman-α forest could be an independent approach to searches based on the SNIa redshift-distance relation, the CMB, BAO, ISW, and gravitational lensing, and one that has received comparatively little attention in the literature.

2. Simulations

Previously Ref. [15] considered the effects on the Lyman-α forest from various values of cosmological constant in the context of a semi-analytic treatment of the Lyman-α forest. In Ref. [5] we expanded upon that work by making use of high-resolution N-body simulations, from which we extracted synthetic Lyman-α spectra. Moreover, we have explored dynamical models of dark energy.

Our simulations were run with the publicly available smoothed-particle-hydrodynamics (SPH) code GADGET-2[16], modified[5] to work with dynamical dark energy.[17] Simulating the Lyman-α forest requires a very high resolution. It has been suggested[18] that a resolution of $\approx 40\ h^{-1}$ kpc in a box of size $L \approx 40\ h^{-1}$ Mpc is needed to adequately resolve the structure of the Lyman-α forest and achieve convergence in the power spectrum. With these requirements in mind, we simulated 1024^3 dark matter particles in a box of length $40\ h^{-1}$ comoving Mpc.

Due to the high resolution requirements of our simulations, we evolve a distribution of only dark matter particles out of consideration for the total run-time. This is justified because in the low-density, mildly non-linear environments typically responsible for the Lyman-α forest, the baryon distribution largely follows that of the dark matter on large scales.[19] Additionally, the effects of non-linear baryonic physics, such as galactic winds, have been shown[20] to be small at large scales where the effects of dark energy should be most prominent.

Our cosmological parameters are those given in Ref. [21]. Other simulation parameters are given in Ref. [5]. We ran five simulations both with a cosmological constant and with various dynamical dark energy where $w(a)$ is the linear slope of the dark energy equation of state with redshift. The dynamical models were chosen such that their parameters were as close to the edges of the allowed 95% confidence range for the (w_0, w_a) parameter space given in the *Planck* analysis.[4] We chose points at the fringes of the allowed parameter space since these models should produce flux power spectra with the largest differences between them. The only exception to this is model DE2-40-1024, $(w_0, w_a) = (-1.1, 1.3)$ which was deliberately chosen from the region of the (w_0, w_a) parameter space that is outside the bounds permitted by *Planck*'s marginalized posteriors. This was done for two reasons: first, we wanted to determine if very extreme values the dark energy parameters were capable of producing a distinct signature in the flux power spectrum of the Lyman-α forest, and second, we were interested in whether or not the flux power spectrum provided constraints on the dark energy parameter space that were in accord with the results determined from other observational probes. The values of w_0 and w_a that we used are $(w_0, w_a) = (-1.0, 0.0), (0.0, -3.0), (-1.1, 1.3), (-2.0, 0.0), (-2.0, 2.0)$.

Each of our simulations was started from the same initial conditions and evolved from $z = 49$ to $z = 2.2$. Our initial conditions were generated using the publicly available second-order Lagrangian perturbation theory code `2LPTIC`[22]. We generated snapshots of each simulation for quasars located at observed redshifts of $z = 4.2, 3.8, 3.0, 2.7$, and $z = 2.2$ as described in Ref. [5]. Our simulations

required on the order of ≈ 10 days on 72 processors to run. Following this, the post-processing took on the order of one week per snapshot, with the majority of the time (about four or five days) being devoted to halo-finding.

3. Implementation of Dynamical Dark Energy

The publicly available version of GADGET-2 assumes that dark energy arises from the cosmological constant. However, we make use of the parameterization given in 5. Nevertheless, modifying GADGET-2 to include the effects of dynamical dark energy was relatively straight forward. Calculating a synthetic spectrum requires knowledge of the densities, temperatures, and HI neutral fractions for each of the simulation particles. Since these are not properties of dark matter particles in GADGET-2, and we ran dark matter only simulations, we calculated these quantities in post-processing. Details of the GADGET calculations and the extraction of the Lyman-α spectra are given in Ref. [5].

The absorption in the Lyman-α forest serves as a way of mapping out the large-scale structure between the observer and the distance source quasar. Thus, the flux power spectrum serves as a proxy for the power spectrum of the underlying matter field that gives rise to the absorption in the Lyman-α forest. Since the matter power spectrum is a measure of the density amplitudes as a function of scale, and these amplitudes depend upon the expansion history of the universe, we can, in principle, use the flux power spectrum to discriminate between dark energy models.

Following Ref. [23], we do not analyze the flux directly but instead consider the quantity:

$$F_p = \frac{e^{-\tau}}{\langle e^{-\tau} \rangle} - 1. \tag{1}$$

F_p is used in place of F because F is sensitive[23] to changes in the mean flux $\langle e^{-\tau} \rangle$. We then take the Fourier transform of F_p using the publicly available package `FFTW3`[a] to calculate the power spectrum. That is, the power spectrum is constructed from the Fourier transform of F_p, which we denote $F_{p,k}$,

$$P_{F_p}(k) = |F_{p,k}|^2. \tag{2}$$

We normalize the spectrum by dividing out the total counts within each bin of frequency k. The frequencies are found via:

$$k_i = \frac{2\pi i}{T}, \tag{3}$$

where i indicates the bin index and T is the period. For discrete Fourier Transforms (DFTs), the signal is assumed to be periodic over the range in which there is data, so the period is simply the length of the spectrum in velocity space.

[a] `http://www.fftw.org/`

4. Results

Using the procedure described in Ref. [5], we extract one-thousand synthetic spectra for each model at each redshift. This pool of spectra was then used to calculate an average power spectrum for each dark energy model at each redshift, along with errors. Figure 1 shows the spectrum through the center of the simulation volume for each of our dark energy models. These are offset from one another for visual clarity. All of the spectra, save for the DE2-40-1024 model, are nearly identical to one another.

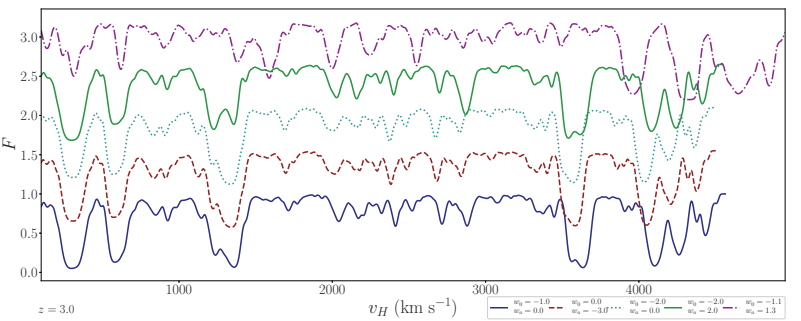

Fig. 1. The synthetic spectrum through the center of the simulation volume for each of our dark energy models at $z = 3.00$. This figure highlights the fact that the spectrum for each of our dark energy models, save for DE2-40-1024 (magenta), are all nearly identical to one another. Each spectrum is offset from the others for reasons of visual clarity.

In order to calculate an average power spectrum at each redshift, we bootstrap a sample of eight-hundred synthetic Lyman-α forest spectra from our pool of one-thousand. The process described in Ref. [5] is then applied to this bootstrapped sample in order to calculate one instance of the power spectrum. This process is then repeated one thousand times to generate one thousand instances of the power spectrum. These instances are then averaged on a k-by-k basis in order to obtain a mean value of P for each k along with a standard deviation, which we take to be the errors on our simulated power spectra.

We applied[5] a k-sample Anderson-Darling (AD) test[24] to analyze the statistical significance of the differences among power spectra. This test places more emphasis on the tails of the distribution. Since dark energy is a large-scale phenomenon, we expect the differences between power spectra to be greatest on the largest scales (smallest k). The key feature of the AD test is the fact that it is distribution-free. This is because the underlying distribution function giving rise to the power spectrum is unknown. With no *a priori* reason to prefer one distribution function over any other, a reasonable place to start is to assume a Gaussian distribution, though we would not necessarily expect this to be the case given that cosmic structure is not normally distributed.

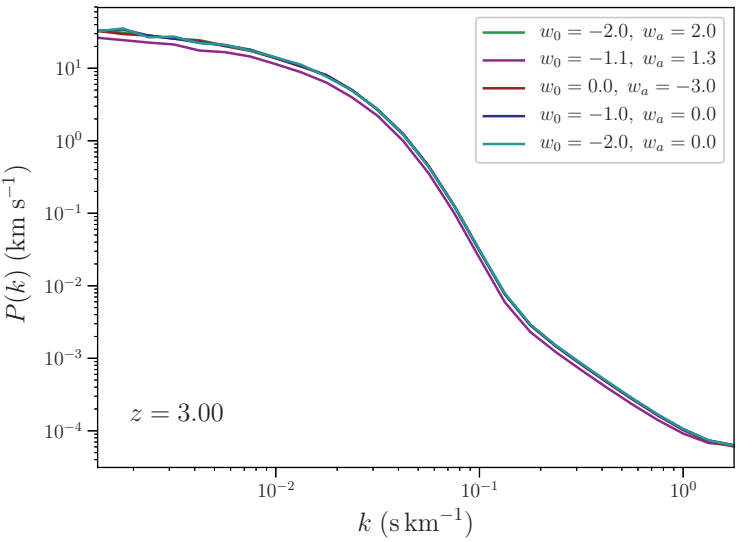

Fig. 2. Power spectrum from each of our dark energy models at $z = 3$. This figure shows that effect of various time-dependent dark energy models on the flux power spectrum of the Lyman-α forest is small.

In summary, his work has explored whether the flux power spectrum of the Lyman-α forest can be used as a probe of time-dependent dark energy. We extracted synthetic Lyman-α forest spectra from high-resolution N-body simulations and used these to calculate the flux power spectrum. We used five different dark energy models, including the cosmological constant and four dynamical, parameterized dark energy models. These models were chosen from the (w_0, w_a) posterior distributions as determined by *Planck*. In particular, of the four dynamical dark energy models we employed, three of them were chosen to lie at the fringes of this posterior, while the fourth was deliberately chosen to lie outside of the 95% C.L. bounds determined by *Planck* to serve as an extreme example from which we might discern an effect on the power spectrum.

Based our pool of synthetic Lyman-α forest spectra, we calculated an average power spectrum for each dark energy model at each redshift. We used k-sample Anderson-Darling test, which shows that there are only marginal differences between the power spectra. Thus, the effects of dark energy on the Lyman-α forest are less significant than the probes based upon the baryonic physics in the IGM. This implies that it is challenging to discriminate among dark-energy models based upon the power spectrum of the Lyman-α forest.

Acknowledgments

This work was supported by the U.S. Department of Energy under grant DE-FG02-95-ER40934.

References

1. Amendola, L., & Tsujikawa, S. 2010, Dark Energy: Theory and Observations (Cambridge: Cambridge Univ. Press).
2. Caldwell, R. R., Dave, R., & Steinhardt, P. J. 1998, PhRvL, 80, 1582.
3. Armendriz-Picn, C., Mukhanov, V., & Steinhardt, P. J. 2000, PhRvL, 85, 4438.
4. Planck Collaboration, Ade, P. A. R., Aghanim, N., et al. 2016b, A&A, 594, A14.
5. J. W. Coughlin, G. J. Mathews, L. A. Phillips, A. P. Snedden & I.-S. Suh, Astrophys. J., 874, 11 (1029).
6. Park, D., & Lee, J. 2007, PhRvL, 98, 081301.
7. Bos, E. G. P., van de Weygaert, R., Dolag, K., & Pettorino, V. 2012, MNRAS, 426, 440.
8. Lee, J., & Park, D. 2009, ApJL, 696, L10.
9. Biswas, R., Alizadeh, E., & Wandelt, B. D. 2010, PhRvD, 82, 023002.
10. Lavaux, G., & Wandelt, B. D. 2010, MNRAS, 403, 1392.
11. Lavaux, G., & Wandelt, B. D. 2012, ApJ, 754, 109.
12. Shoji, M., & Lee, J. 2012, arXiv:1203.0869.
13. Cen, R., Miralda-Escud, J., Ostriker, J. P., & Rauch, M. 1994, ApJL, 437, L9.
14. Bi, H., Ge, J., & Fang, L.-Z. 1995, ApJ, 452, 90.
15. Viel, M., Matarrese, S., Theuns, T., Munshi, D., & Wang, Y. 2003, MNRAS, 340, L47.
16. Springel, V. 2005, MNRAS, 364, 1105.
17. Dolag, K., Bartelmann, M., Perrotta, F., et al. 2004, A&A, 416, 853.
18. McDonald, P. 2003, ApJ, 585, 34.
19. Meiksin, A., & White, M. 2001, MNRAS, 324, 141.
20. Bertone, S., & White, S. D. M. 2006, MNRAS, 367, 247.
21. Planck Collaboration, Ade, P. A. R., Aghanim, N., et al. 2016a, A&A, 594, A13.
22. Scoccimarro, R., Hui, L., Manera, M., & Chan, K. C. 2012, PhRvD, 85, 083002.
23. Hui, L., Burles, S., Seljak, U., et al. 2001, ApJ, 552, 15.
24. Anderson, T. W., & Darling, D. A. 1952, Ann. Math. Statist., 23, 193.